# Multi-Spectral Image Analysis for Improved Space Object Characterization

**Michael J. Duggin[a], Jim F. Riker[a], William Glass[a], Keith A. Bush[c], David Briscoe[d], Meiling Klein[d], Mark L. Pugh[b] and Brian Engberg[a]**

[a]Air Force Research Laboratory
Space Vehicles Directorate
3550 Aberdeen Avenue SE
Kirtland AFB, NM 87117
USA

[b]Air Force Research Laboratory
Information Directorate
525 Brooks Road
Rome, NY 13441

[c]Schafer Corp
2309 Renard place, SE, Suite 300
Albuquerque, NM 87106
USA

[d]Northrop Grumman Corp
2600 Yale Blvd SE
Albuquerque
NM 87106

Michael.duggin@kirtland.af.mil

**ABSTRACT**

*The Air Force Research Laboratory (AFRL) is studying the application and utility of various ground-based and space-based optical sensors for improving surveillance of space objects in both Low Earth Orbit (LEO) and Geosynchronous Earth Orbit (GEO). At present, ground-based optical and radar sensors provide the bulk of remotely sensed information on satellites and space debris, and will continue to do so into the foreseeable future. However, in recent years, the Space Based Visible (SBV) sensor was used to demonstrate that a synthesis of space-based visible data with ground-based sensor data could provide enhancements to information obtained from any one source in isolation. The incentives for space-based sensing include improved spatial resolution due to the absence of atmospheric effects and cloud cover and increased flexibility for observations. Though ground-based optical sensors can use adaptive optics to somewhat compensate for atmospheric turbulence, cloud cover and absorption are unavoidable. With recent advances in technology, we are in a far better position to consider what might constitute an ideal system to monitor our surroundings in space. This work has begun at the AFRL using detailed optical sensor simulations and analysis techniques to explore the trade space involved in acquiring and processing data from a variety of hypothetical space-based and ground-based sensor systems. In this paper, we briefly review the phenomenology and trade space aspects of what might be required in order to use multiple band-passes, sensor characteristics, and observation and illumination geometries to increase our awareness of objects in space.*

---

| 1. REPORT DATE **SEP 2008** | 2. REPORT TYPE | 3. DATES COVERED **00-00-2008 to 00-00-2008** |
|---|---|---|
| 4. TITLE AND SUBTITLE **Multi-Spectral Image Analysis for Improved Space Object Characterization** | | 5a. CONTRACT NUMBER |
| | | 5b. GRANT NUMBER |
| | | 5c. PROGRAM ELEMENT NUMBER |
| 6. AUTHOR(S) | | 5d. PROJECT NUMBER |
| | | 5e. TASK NUMBER |
| | | 5f. WORK UNIT NUMBER |
| 7. PERFORMING ORGANIZATION NAME(S) AND ADDRESS(ES) **Air Force Research Laboratory,Space Vehicles Directorate,3550 Aberdeen Ave SE,Kirtland AFB,NM,87117** | | 8. PERFORMING ORGANIZATION REPORT NUMBER |
| 9. SPONSORING/MONITORING AGENCY NAME(S) AND ADDRESS(ES) | | 10. SPONSOR/MONITOR'S ACRONYM(S) |
| | | 11. SPONSOR/MONITOR'S REPORT NUMBER(S) |

12. DISTRIBUTION/AVAILABILITY STATEMENT
**Approved for public release; distribution unlimited**

13. SUPPLEMENTARY NOTES
**2008 Advanced Maui Optical and Space Surveillance Technologies Conference, 16-19 Sep, Maui, HI.**

14. ABSTRACT

**The Air Force Research Laboratory (AFRL) is studying the application and utility of various groundbased and space-based optical sensors for improving surveillance of space objects in both Low Earth Orbit (LEO) and Geosynchronous Earth Orbit (GEO). At present, ground-based optical and radar sensors provide the bulk of remotely sensed information on satellites and space debris, and will continue to do so into the foreseeable future. However, in recent years, the Space Based Visible (SBV) sensor was used to demonstrate that a synthesis of space-based visible data with ground-based sensor data could provide enhancements to information obtained from any one source in isolation. The incentives for space-based sensing include improved spatial resolution due to the absence of atmospheric effects and cloud cover and increased flexibility for observations. Though ground-based optical sensors can use adaptive optics to somewhat compensate for atmospheric turbulence, cloud cover and absorption are unavoidable. With recent advances in technology, we are in a far better position to consider what might constitute an ideal system to monitor our surroundings in space. This work has begun at the AFRL using detailed optical sensor simulations and analysis techniques to explore the trade space involved in acquiring and processing data from a variety of hypothetical space-based and ground-based sensor systems. In this paper we briefly review the phenomenology and trade space aspects of what might be required in order to use multiple band-passes, sensor characteristics, and observation and illumination geometries to increase our awareness of objects in space.**

15. SUBJECT TERMS

| 16. SECURITY CLASSIFICATION OF: | | | 17. LIMITATION OF ABSTRACT | 18. NUMBER OF PAGES | 19a. NAME OF RESPONSIBLE PERSON |
|---|---|---|---|---|---|
| a. REPORT<br>**unclassified** | b. ABSTRACT<br>**unclassified** | c. THIS PAGE<br>**unclassified** | **Same as Report (SAR)** | **14** | |

## 1.0   INTRODUCTION

The Air Force has requirements for surveillance of objects in space in near real time. This is a highly complex many-body problem.  Modern reliance on space by the US military requires that we have immediate and continuing information on space objects throughout a spherical volume extending beyond geosynchronous orbit ($3.5 \times 10^4$ km radius).  This translates to a volume of approximately $2 \times 10^{14}$ km$^3$.  Within this volume are communication, GPS, weather, and other space assets vital to our economy and national security.  We need to be aware of the health of these craft, and to be aware of potential degradations that might occur due to, for example, solar events.  In contrast, during the World War II Battle of Midway, the volume that could possibly be occupied by opponent aircraft and surface vessels was approximately $1,000 \times 1,000 \times 5$ km $= 5 \times 10^6$ km$^3$.  Thus, the required surveillance volume in modern times is $4 \times 10^7$ times larger than the volume occupied by opposing forces during the Battle of Midway.  An added complication to the Battle of Midway is that the objects requiring detection at that time were quite large (battleships, aircraft carriers) whereas the objects that we are potentially interested in today could be quite small. This includes space debris that could, for example, damage the Space Station. Thus, what is needed is the ability to be aware of small objects within an extremely large spatial volume.

Space-based optical sensing of space objects may provide some unique benefits compared to more traditional ground-based methods. One obvious benefit is potentially improved spatial resolution due to the absence of atmospheric effects and cloud cover.  Space-based sensing may also benefit from a wider range of available sensing geometries than is available from ground sensors.  Ground-based sensors are constrained to view the side of the satellite facing the earth, providing little information on the status of other portions of the craft.  In many cases, the earth facing side is of great interest as important payloads such as communication equipment are commonly pointed toward the earth.   However, we can't rule out the possibility that future spacecraft will focus payloads away from the Earth.  Also, for a more complete assessment of spacecraft function, condition and status, space-based sensing may provide viewing opportunities rarely presented to a ground sensor.  This can be an important capability in resolving anomalies such as the failure of a solar panel to deploy, as occurred with Skylab. Space sensors may also offer additional flexibility in timeliness and geometry, whereas a ground-based sensor may be consistently constrained waiting for a satellite pass or for a diminution of cloud cover.

Space-based optical sensing of space objects also presents some unique challenges. Accurate radiometric calibration of recorded image data and transmission of the data to the ground for analysis are two challenges unique to space-based sensors. The best approach to calibrating space-based sensors to ensure accurate image phenomenology in currently unclear.  Recorded image data may be constrained by on-board processing capabilities and the bandwidth available for satellite downlink.  We need to understand the most economic data set that will be adequate to solve our space sensing problems (e.g. detection, characterization and changes in satellite health).  Clearly, we also need to understand the phenomenology of space-based imagery.  One example is imagery containing solar "glints." Glints might be helpful for object detection, but will produce sensor saturation in electronic FPA sensors resulting in a "white out" condition for many of the pixels representing a space object. Careful mission planning is important to decide which space objects to observe, and with what view and illumination geometry, sensor parameters, band-passes, etc., to obtain useful space-based imagery.

The Space-Based Visible (SBV) Electro-Optical (EO) sensor system[1] added a space-based component to ground-based systems for space surveillance. Over its successful decade of life, it

demonstrated that a synthesis of space-based visible data with ground-based EO data could provide information that was more useful than information from any one source in isolation. It could do several things that ground-based systems cannot, such as look at most of the geosynchronous belt without having to be limited by clouds, atmospheric turbulence or long atmospheric path lengths. Besides SBV, some work was done to investigate the possible "dual-use" capability of sensors such as the panoramic view Solar Mass Ejection Imager (SMEI). Nonetheless, this was exploratory, and while SBV could only see visual magnitude objects of +17 when new (it degraded with time), SMEI was even less capable. As a hypothetical basis for comparison, in order to detect a Lambertian 100 cm$^2$ object of albedo 0.2 (about the size of typical small satellites launched by several universities) at 3.7 X 10$^7$ m range, it is necessary to have a radiometric resolution of a visual magnitude +20 or better (ignoring atmospheric degradation). Therefore, we would ideally need a sensor with a substantially greater radiometric sensitivity than SBV to be capable of recording small objects at GEO if the sensor was (as was the case with SBV) to be located in LEO.

Two drawbacks to space-based sensors may be cost and accessibility. To build, launch and operate a space-based sensor could be many times the cost of a ground-based counterpart. Space-based sensors may also be difficult or impossible to service. An example is the cost associated with the Hubble Space Telescope (HST) servicing missions. Thus, to make a space-based surveillance system feasible, it must be reliable and collect timely, high quality data of possibly small and low-albedo space objects to provide significant advantages over well-tested ground-based telescope systems. Trade-off studies concerning various aspects of optical sensor design (such as telescope size, optical design, and camera sensitivity) and overall satellite system considerations (such as longevity and launch costs) are clearly needed. Modelling and Simulation (M&S) of potential space-based imaging scenarios together with the application of image analysis techniques to simulated imagery is a cost-effective approach to understanding the space-based imaging phenomenology that affects optical sensor design. AFRL is currently engaged in M&S studies of such scenarios to develop a detailed, physics-based understanding of space object imaging, and to consider the ramifications of sensor parameter and tasking parameter trades[2]. These M&S studies are being performed using the Time-domain Analysis Simulation for Advanced Tracking (TASAT) software[3-6] developed by the Air Force for detailed design and assessment of optical imaging and tracking systems used in various Air Force applications.

## 2.0 Space Object Sensing Geometries

To understand the scope the problem of developing an awareness of space objects, we need to consider that there are over 12,000 objects 10 cm or larger in size that we can currently track in earth orbit. As discussed above, these satellites (alive or dead) and debris are distributed over a very large volume. In order to derive useful information, we need to be able to both detect and characterize objects within this volume. This task becomes more complex as spatial resolution is reduced either by distance or diminished object size. For example, most objects in geosynchronous orbit (GEO) are at least 36,000 km distant and may only subtend less than one instantaneous field of view (IFOV) at the focal plane (and therefore be completely spatially unresolved).

Trade space studies are useful for determining system capabilities required for various imaging scenarios. The minimum sensor capabilities required to observe a 100 cm$^2$ space object from Earth under ideal conditions for various albedos and ranges (specified in terms of required stellar magnitude detection) are shown in figure 1. The curves indicate that observations of an object in geosynchronous-orbit require a sensor with at least a +19 visible magnitude capability to perform even a marginal detection for most albedos. When atmospheric turbulence (for a ground-based

sensor) and sensor noise are considered, this requirement becomes larger. Of course, spatial resolution is also aperture size and band-pass dependent as shown by the curves in figure 2. Shorter wavelengths (such as in the UV) allow for smaller apertures to obtain the same imaging resolution. This is a significant advantage to developing and deploying a space-based system. Simplified trade space studies, such as these, are useful in determining the minimum system requirements for a given space object imaging scenario. Extended trade studies are required to determine the effects of sensor noise, optical limitations, atmospheric turbulence, and various other factors on system performance and benefits to space surveillance missions. Also, the possibility of combining data obtained with different sensors, at different times, with different band-passes and modalities, and from different vantage points is being considered to enhance the information provided by a single sensor observation.
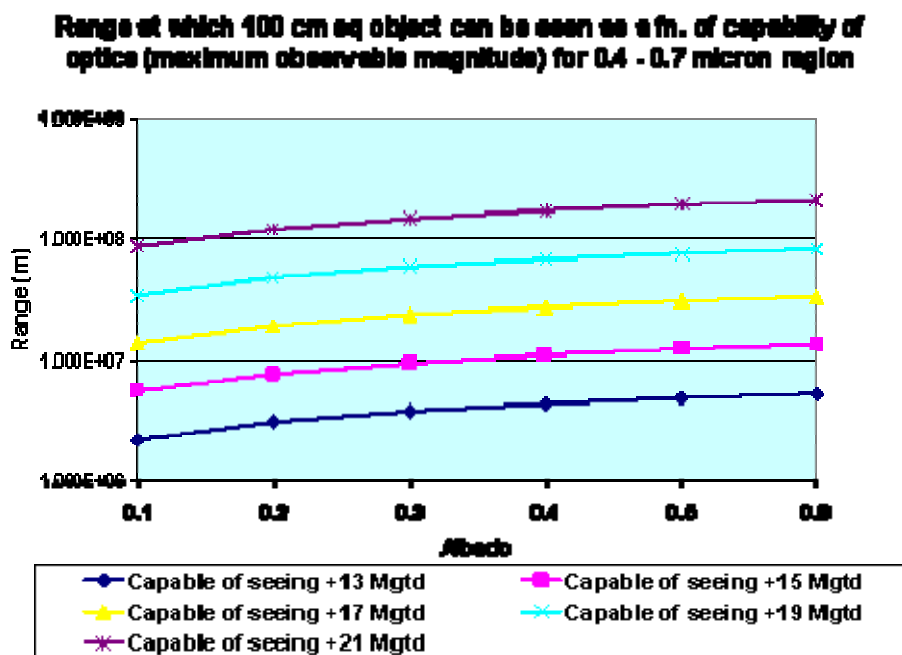


Figure 1. Trade space studies showing detection capability needed for 100 cm$^2$ space objects of various albedos at various ranges.

**Range at which 10 cm spatial resolution possible for different apertures
in several bandpasses**



*UV offers increased spatial resolution We can get almost the same spatial resolution in the UV with a 1.0m diameter*
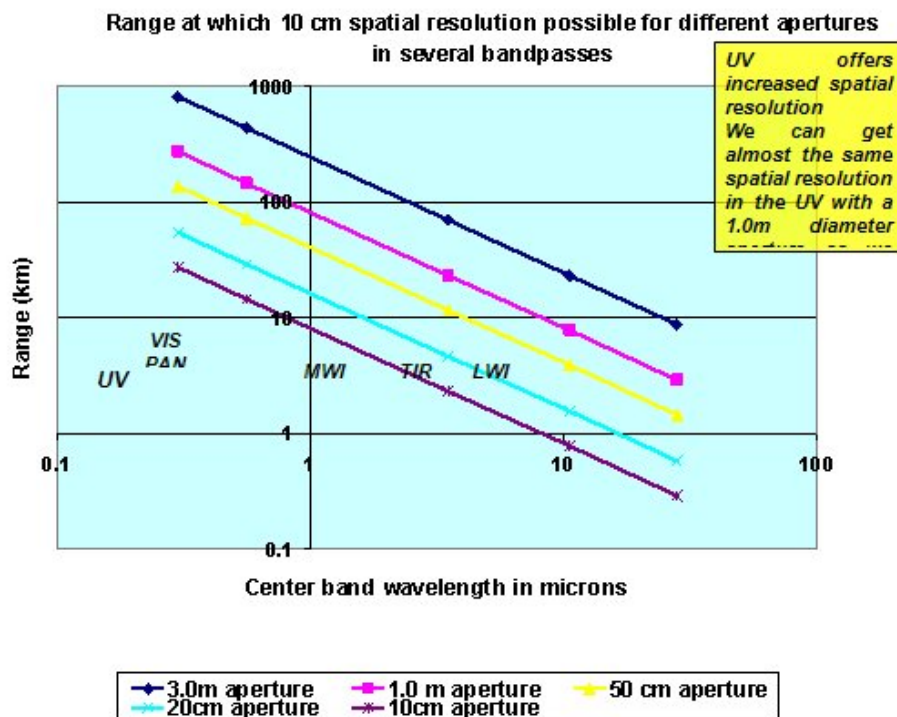
Figure 2. Bandpass-dependence of spatial resolution from the UV to the thermal IR

## 3.0 SIMULATION AND MODELING

Simulation and modelling of space object optical surveillance scenarios requires knowledge of object and observation platform trajectories, object illumination conditions and optical scattering properties, and observer optical system specifications. Given a Two-Line-Element (TLE) set or precision state vector for a satellite or object of interest, we can investigate detection capabilities from Earth or from a notional observing satellite to seek the optimal conditions for observation. An observing satellite platform could be located in Low-Earth-Orbit (LEO), Mid-Earth-Orbit (MEO), Highly Elliptical orbit, or Geosynchronous-Earth-Orbit (GEO), depending on the problem under consideration. Observer satellite orbital parameters and attitude must be known precisely relative to the Earth, Moon, and Sun to determine optimal observation opportunities for objects of interest and to avoid direct viewing into the Sun. Precise object models are also required to accurately represent the radiometric scattering for a given imaging scenario and allow for proper design of an observer optical imaging system. The AFRL TASAT simulation provides the modeling and simulation platform needed to conduct space object imaging simulations that meet these requirements. TASAT has capabilities for satellite orbit modelling, object optical scattering, and observer optical system modelling when provided object and observer orbit information and detailed object models for imaging scenarios of interest.

TASAT was first developed for performing detailed simulations of LEO satellite, passive and active, ground-based, tracking and imaging systems.[1,3,4] TASAT has evolved to allow simulation of imaging scenarios with space-based imaging and illuminator platforms for both passive (solar, lunar, earthshine) and active (laser) satellite illumination. TASAT provides radiometrically sensitive 2D renderings of detailed 3D Computer Aided Design (CAD) satellite models in simulated Earth orbits.

The renderings are performed using ray tracing techniques and a database of satellite material optical properties. Each element of the 3D CAD model has its own material properties, so that appropriate optical, polarization, and scattering effects may be applied to each surface. Rendered image fields are then convolved with the imaging system Point Spread Function (PSF) and degraded with sensor spatial sampling and noise models to provide realistic satellite imagery for the defined scenario as a function of simulation time.

TASAT uses a library of the spectral optical properties of satellite materials, known as the satellite materials database, to model satellite object radiometry for a given observation scenario. These materials are measured at various wavelengths and stored in terms of optical quantities such as spectral reflectivity and bidirectional reflectance function (BRDF) values for a limited number of wavelengths. However, there are gaps in the database where materials measurements are needed to provide more consistent and accurate modelling of satellite materials optical properties. Currently, both empirical and semi-empirical models are used to predict the geometric behaviour of the optical properties with varying view and illumination geometry. The Maxwell-Beard[5] BRDF model is used in TASAT to simulate 3D material scattering from limited BRDF measurements. This model, while accurate for many materials, has been shown to decrease in accuracy for materials with very specular scattering. It is well-documented that our understanding of the geometric behaviour of these optical properties is imperfect, and that our knowledge of how the optical properties of satellite materials vary in a space environment is limited.

Efforts are underway to match observed and calculated spectral radiant power from each facet of space objects (using ground-based telescope observations and TASAT simulations of these observations) making it possible, in an iterative process, to more accurately predict the nature of the optical properties of the materials and provide more accurate predictions of object observations. We are also currently engaged in satellite pre-launch measurements that will increase our understanding of the accuracy and reproducibility of TASAT predictions. The optical properties of spacecraft materials are also affected by space aging (weathering). These effects are not included in laboratory BRDF data. It is expected that, among other optical changes, aging might dramatically reduce solar glints. The development of a space-aging model for the optical properties of spacecraft materials could therefore greatly improve the accuracy of some model predictions.

TASAT ray tracing, 3D model geometry and materials properties determine the average power received per pixel, and is described as follows.

$$P_{received}(i,j) = J \cdot A_{pixel} \cdot \Omega_{receiver} = I_o \cdot \cos(\theta_i) \cdot BRDF(\theta_i, \theta_r) \cdot A_{pixel} \cdot \Omega_{receiver}$$

Where:

$W_{receiver}$ = receiver solid angle, J - directional radiance (w/m$^2$-sr)

$A_{pixel}$ = pixel surface area

$BRDF$ = bidirectional reflectance distribution function

$I_0$ = unit irradiance (w/m$^2$)

$\theta_i, \theta_r$ =incident and reflected ray angles

$$BRDF(\theta_i, \varphi_i, \theta_r, \varphi_r) = R_x(\beta) \cdot \frac{\Xi(\alpha)}{4 \cdot \cos(\theta_i) \cdot \cos(\theta_r)} \cdot SM_o$$

$R_x(b)$ = first surface Fresnel reflec. (x is "p" or "s")

$\Xi(\alpha)$ =micro-facet tilt distribution function

$SM_0$ =shadow masking function (bi-static scenarios)

Bush, *et. al.*[6,7] have also used the TASAT model to make simulation predictions with polarization scattering effects. TASAT produces 2D polarization renderings using the same detailed 3D object models, ray tracing techniques, and database of object material optical properties together with the Fresnel equations to model the surface and bulk polarization effects. Renderings are obtained assuming an ideal uniform illumination of the object with a specific polarization state and with unit irradiance (i.e., one watt per meter squared). Object material optical properties, from the materials database, are assigned to each element of the model so that appropriate optical, polarization and scattering effects may be applied for each material. Complete polarization renderings may be obtained either in terms of scattered Stokes parameter fields or as scattered X and Y polarized intensity component fields, relative polarization vector retardance, and a depolarized intensity field.

## 4.0 SIMULATION RESULTS AND ANALYSIS

TASAT has been used to provide space-based imaging simulation results using 3D CAD satellite models for the Hubble Space Telescope (HST) and the Defence Meteorological Satellite Program (DMSP) Flight 8 (F-8) satellites. TASAT imaging results using these models have been calibrated radiometrically, for limited scenarios, using observational data from the 3.6 m telescope at the Air Force Maui Optical Site (AMOS) through comparison with model predictions. The calibrated models were then used to simulate a 33-band image set in order to study the effects of band-pass, viewing and illumination geometry, and range on predicted radiometric image fidelity. For very large range observations, producing unresolved imagery, multi-spectral analysis has also been used to illustrate possible approaches for satellite discrimination using only unresolved image data. Results and analysis from these efforts is provided below.

Figure 3 shows pristine images calculated for the DMSP satellite at spectral wavelengths between 400 nm and 15 $\mu$m. The images in Figure 4a show that the DMSP solar panel provides low radiometric scattering relative to the DMSP body in the visible wave-bands and more significant scattering in the Ultra-Violet (UV – 400 nm) and in the Near-Infra-Red (Near-IR – 1050 to 2450 nm) wave-bands. DMSP body details observed in the images also vary with wave-band. This is particularly noticeable in the transition from UV to Visible observation and in the transitions from NIR to Mid-IR and then to Far-IR wave-bands. If we consider the degradation introduced by a diffraction-limited optical system for a range of approximately 750 km, we can see from Figure 4 that there is a considerable degradation beyond a spectral range of 2 $\mu$m and approaching the "barely resolved" condition at 13 $\mu$m. Clearly, diffraction degrades the spatial resolution of the image significantly as wavelength increases so that, even though useful radiometric information might exist at longer wavelengths, there is increased difficulty in gaining useful spatial information at longer wavelengths. Of course, including the effects of the focal plane array and residual atmospheric blurring will further degrade the imagery.
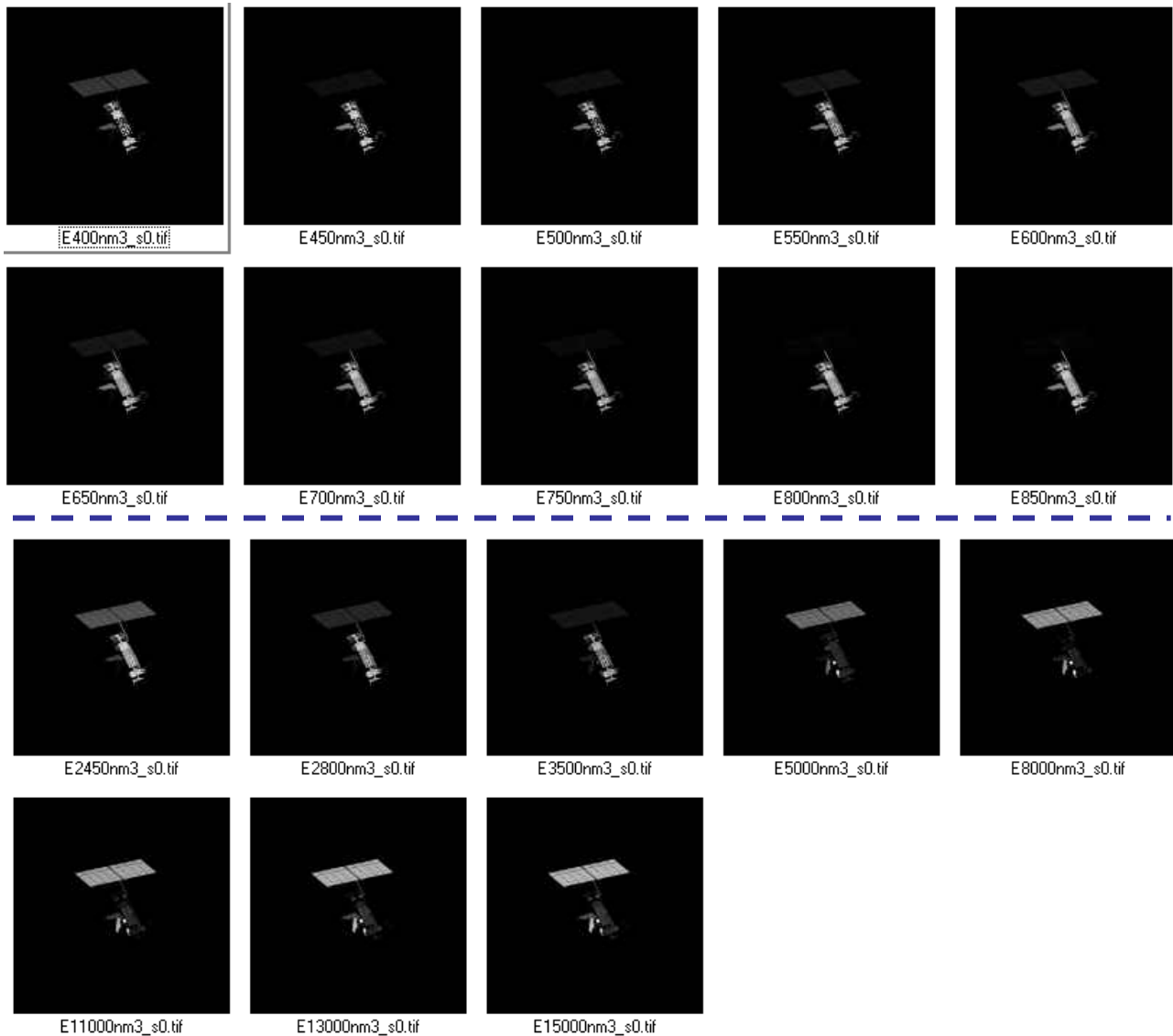
*Figure 3. The DMSP satellite viewed for a solar phase angle of 40$^o$. The images shown are calculated for wavelengths between 400 nm and 15.0 $\mu$m and have not been modulated by optics, focal plane electronics, or the atmosphere. Images for 900 through 1050 nm (not shown) are similar to the visible images and images for 1100 through 2100 nm (not shown) are similar to the image shown at 2450 nm*

NASA images of the HST shown in Figure 5 clearly show wrinkles present in multi-layered insulation (MLI) material that needs to be accounted for in TASAT to provide accurate radiometric modelling. The image shown in the middle of Figure 5 was enhanced using a convolution filter to more clearly show the wrinkles. Material wrinkles cause the BDRF behaviour to be different from completely specular or diffuse surfaces. TASAT uses a statistical "texture map" approach to accurately model the statistics of the wrinkled MLI. The simulated HST image on the right in Figure 5 illustrates the results of this rendering process. Predicted TASAT simulation images of the HST (also showing texture mapping effects) are shown in Figure 6 for one particular solar phase angle at three different wavelengths (1.05 $\mu$m, 5.5 $\mu$m and 12.5 $\mu$m) to illustrate TASAT capabilities.

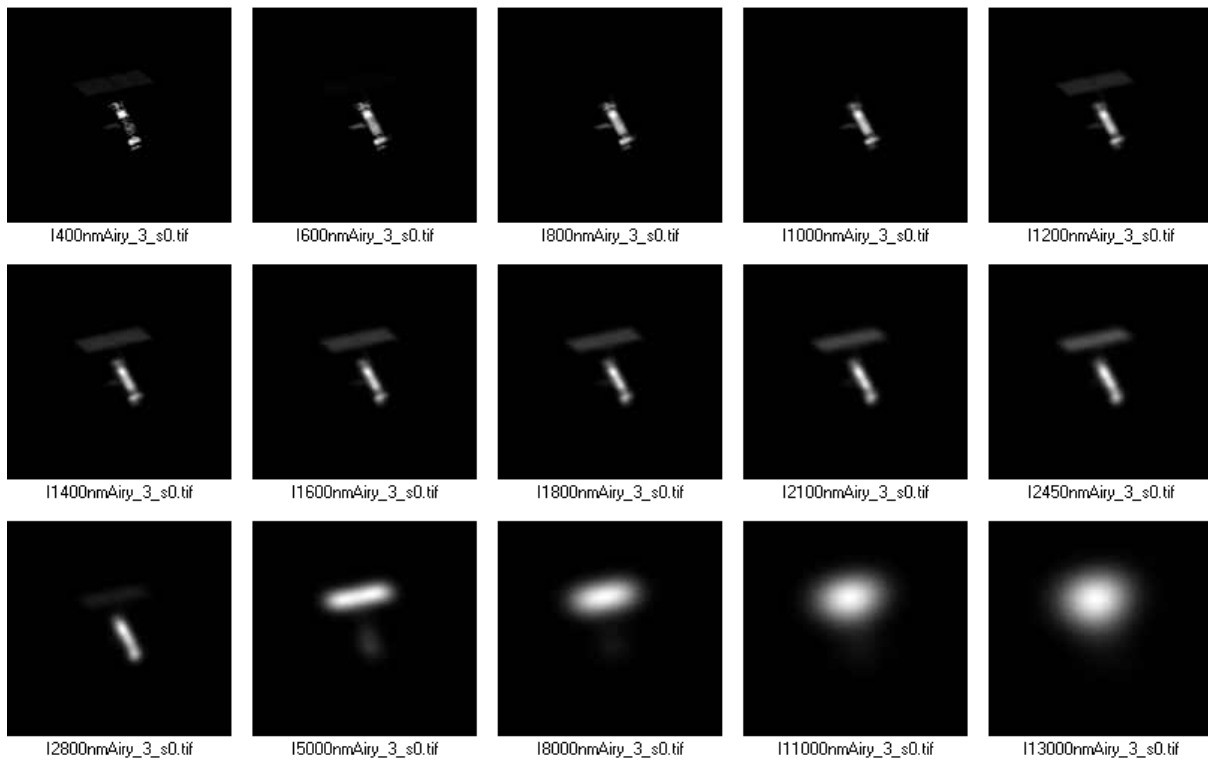*Figure 4. The DMSP satellite viewed for solar phase angle of 40$^o$. The images shown are calculated for wavelengths between 400 nm and 13.0 $\mu$m and have been modulated by diffraction limited optics.*
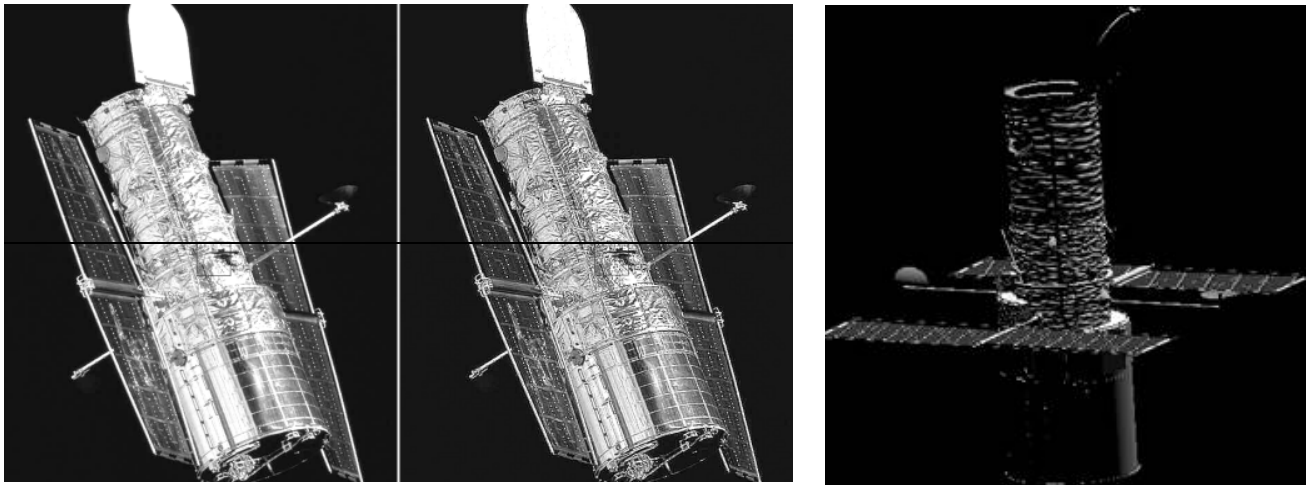


*Figure 5. The Hubble Space Telescope, prior to the 1997 refurbishment of the solar panels. The wrinkled multi-layer insulation (MLI) on the telescope tube is clear in the image on the left, but may be easily enhanced using a simple convolution filter, as shown in the middle image.  The image on the right is a TASAT simulated image.*
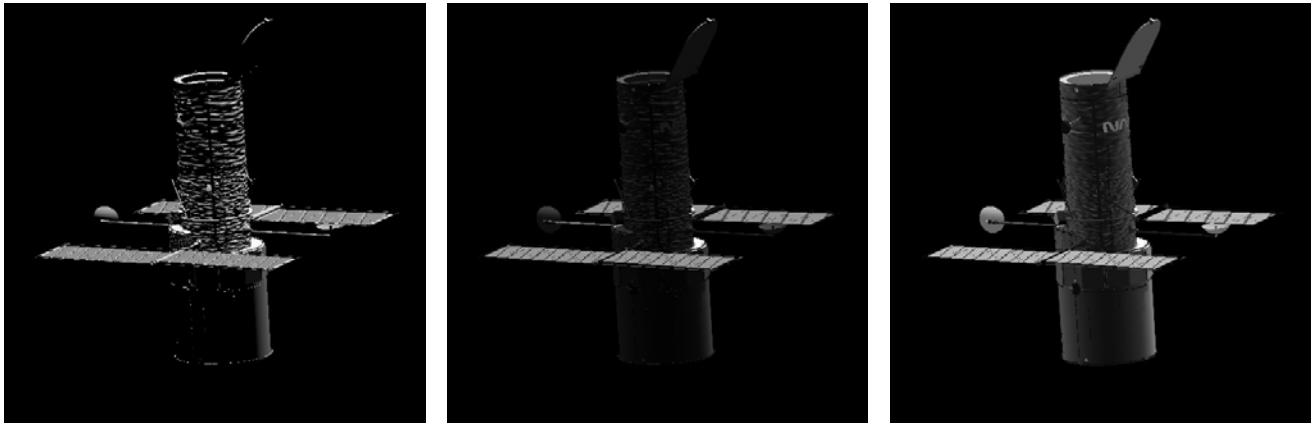
*Figure 6. Simulations of the Hubble Space telescope at (left to right) 1.05 µm, 5.5 µm and 12.5 µm*

Figure 7 shows several outputs from TASAT in a simulated satellite-to-satellite imaging scenario. Here, DMSP F8 is simulated for three ranges. Simulations should also include factors such as pointing accuracy and stability, spectral filters, integration time, zoom lens settings and so on. Such factors can be critical, and it is important to consider them in determining image-by-image how these factors might impact acquired data. For example, it is well known that glints can cause the integration time for a sensor to adjust such that useful information is compressed into the lower part of the dynamic range, thereby reducing image utility.
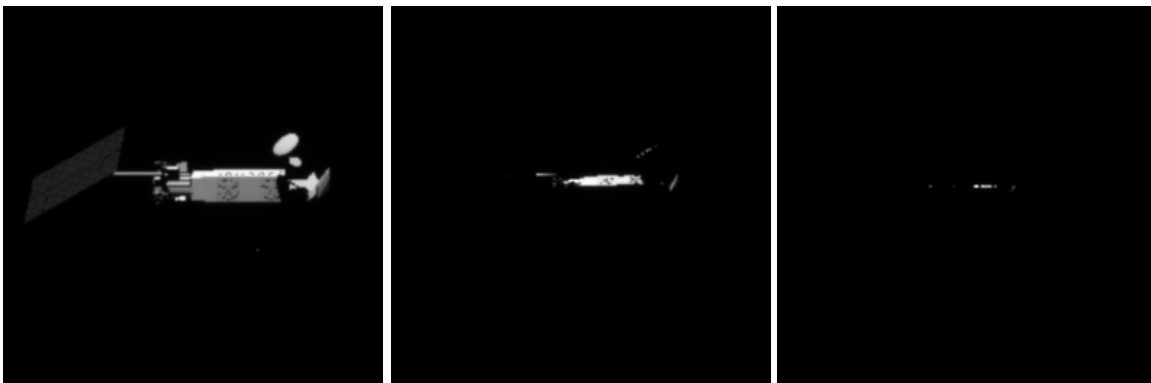


*Figure 7. Space-Based TASAT image simulation of DMSP at increasing ranges*

It is possible that additional spectral radiometric information may be contained within some linear combination of spectral band-pass images. This possibility is explored by reviewing the principal component images of the DMSP (F-8) satellite shown in figure 8. Here, the panchromatic image is compared with images resulting from Principal Component Analysis (PCA) of the waveband-dependent images. PCA images contain information from all 33 band-passes in just a few images, so that considerably more image detail can be seen than in the single wide-band panchromatic image. PCA analysis is a common technique used for reducing multidimensional data to a more manageable reduced set, while preserving information content.
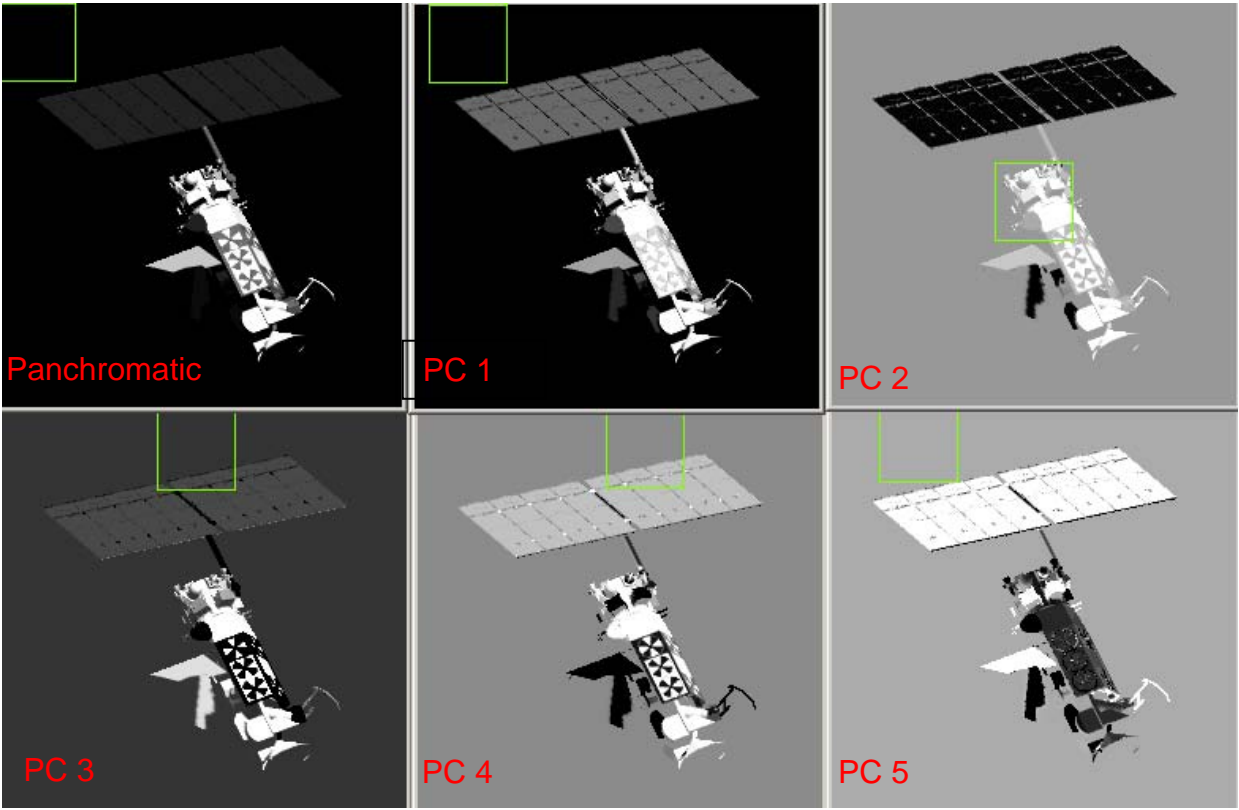
*Figure 8. A simulated panchromatic image, and the first five principal components of the 33 multi-spectral image dataset. It is seen that the additional wavebands add new information that is not seen in the panchromatic image.*

Several approaches have been considered for the analysis of unresolved imagery from TASAT (including PCA analysis) in the interest of developing techniques for discriminating space objects from long observation ranges.

Recent analysis efforts indicate that PCA image analysis may also be useful for identifying unresolved differences in FPA image collections of multi-spectral data. Simply plotting pixel values of the PCA images from one space object versus another can provide some interesting contrasts in data behaviour, yielding information on the similarity of the space objects. This is illustrated in Figure 9 for two very similar (GORIZONT and EKRAN) and two very different (Hubble Space Telescope: HST and DMSP F-8) satellites. The two similar satellites exhibit a linear behaviour in plotting the PCA values against each other, whereas the two different satellites exhibit a scattering of PCA image values when plotting PCA values against each other. Also shown in the Figure are the image sums versus wave-band for each case. The corresponding similarities and differences between these satellites are also evident in these plots as a function of wave-band.

Performing image correlations of unresolved images as a function of wave-band may also provide information for discriminating space objects. Figure 10 shows the relative unresolved image averages as a function of wave-band for five different satellites as well as the average normalized correlation between the satellite FPA images over wave-band at two different solar phase angles (SPA = 12 degrees and 170 degrees). The relative averages vary with the amount of scattered light for each satellite at each wavelength. GORIZONT, RADUGA, and EKRAN are similar satellites in

terms of satellite bus structure and DMSP and HST are very different from each other and from the other three satellites. At a 12 degree solar phase angle most of the correlations are rather high, but may distinct enough to allow discrimination. GORIZ and EKRAN are indistinguishable, having identical correlations with the other satellite images and very similar wave-band energy distributions. At SPA = 170 degrees, significant glints occur in the imagery of all of the satellites with HST producing glints containing significantly more energy than the others as shown in the relative average wave-band distributions. The relative correlation differences between satellites are significantly different at 170 degrees, possibly allowing for satisfactory discrimination of these satellites under these conditions.
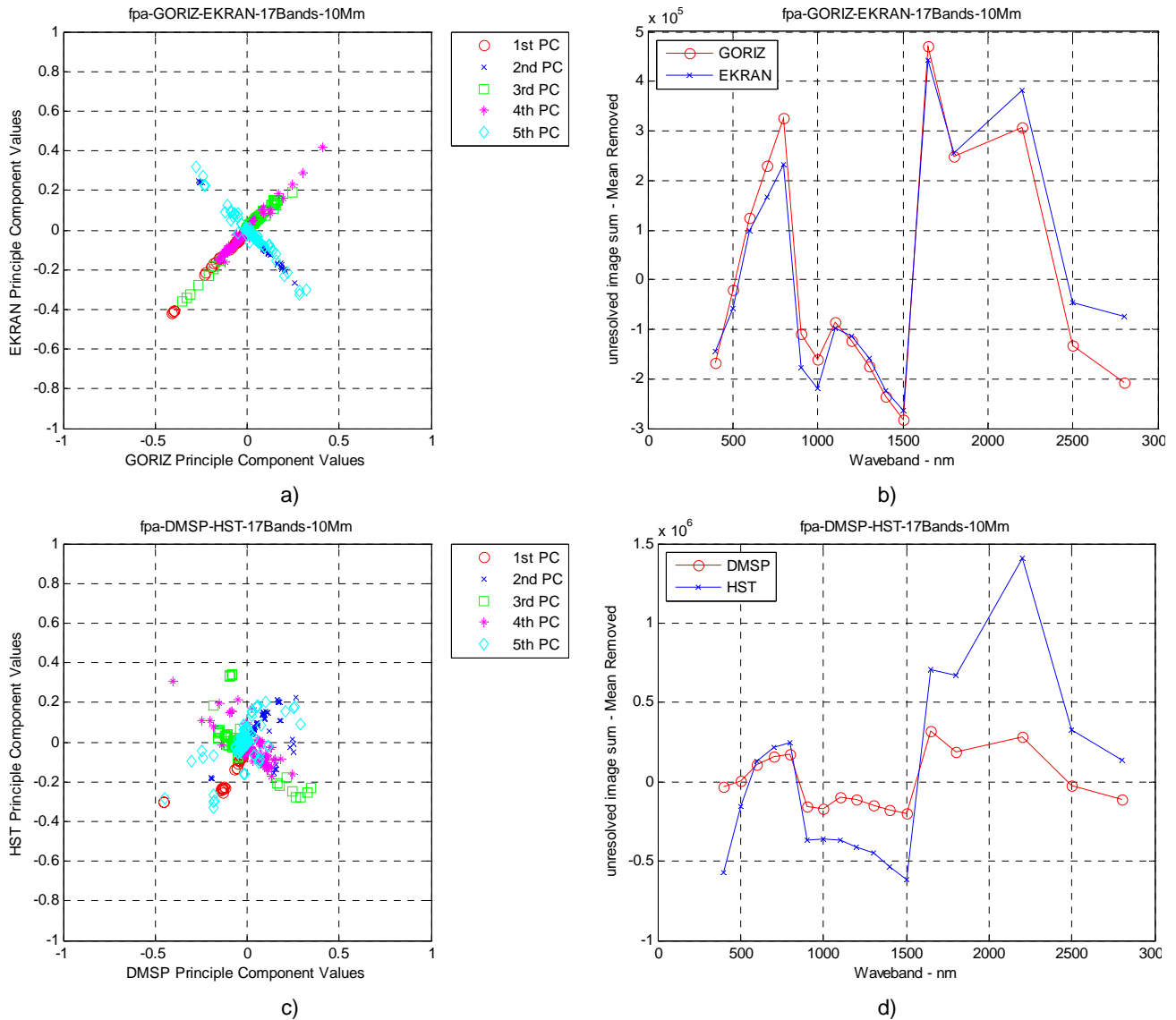


*Figure 9. Unresolved imaging analysis for space object discrimination: plots of FPA image pixels from PCA of two different satellites (a) and c)) and plots of FPA image sums versus wave-band (b) and d)); satellites in a) and b) have similar satellite buses; satellites in c) and d) have very different satellite buses (DMSP and HST).*
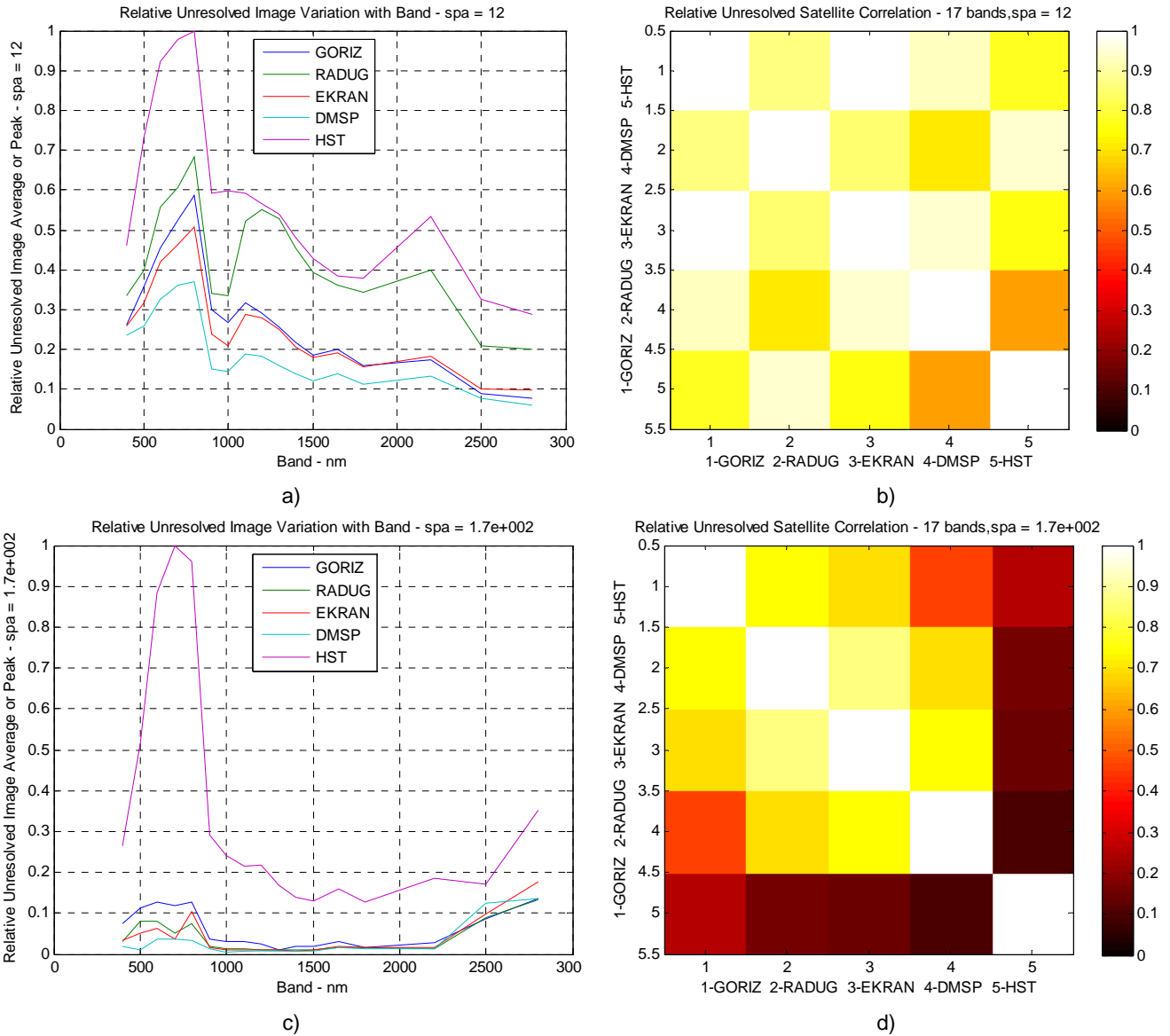
*Figure 10. Unresolved imaging analysis for space object discrimination: plots of relative FPA image average for 5 different satellites versus wave-band (a) and c)) and images showing FPA correlation between 5 different satellites averaged over waveband (b) and d)); a) and b) are for solar phase angle = 12 degrees; c) and d) are for solar phase angle = 170 degrees.*

Processing of image data is sensor specific and the complexity of the algorithms used may vary with the surveillance task. For panchromatic images, little or no processing may be implemented. Other image processing techniques such as sharpening filters may also be considered. An analysis of data from more complex sensors will more complex algorithms. Examples include LWIR imaging where complicated fixed pattern noise and backgrounds can be troubling and are generally "processed out" with the application of gain and offset in a non-uniformity correction. These calculations may be accomplished at a faster rate by using a 64-bit processor computer. However, we are currently expecting to be substantially more efficient in exploring the parameter space (to

better understand the phenomenology) by implementing processing techniques on a supercomputer at the Maui High Performance Computing Center (MHPCC).

## 5.0 CONCLUSIONS

Space-based optical sensing of space objects may provide some unique benefits to space surveillance operations; such as an absence of atmospheric degradation and clouds in observations. Also, space sensors aren't limited to operations within terrestrial atmospheric transmission windows, allowing for viewing possibilities in other potentially useful wavelength bands (such as in the UV). Therefore, all of those bands that might be helpful in the characterization procedure can potentially be used. Understanding of space object phenomenology (such as object surface "glints") is enabled by the TASAT predictive model through the prediction of space object images with radiometric accuracy.

Through TASAT simulation efforts, we are working to develop a physics-based, detailed understanding of the imaging of space objects. Our approach to developing our knowledge base is to predict image data for differing scenarios and for a wide range of optical sensors (visible to long-wavelength infrared) and to perform analysis on the imagery to determine the best approaches for exploiting image information. Currently we are using existing simulation codes, models and data to predict images under certain engagement scenarios, obtained for a variety of view and illumination geometries, and recorded by sensors with various spectral band-passes, responses and focal plane characteristics. Initial results have confirmed the need for a careful, organized approach to understanding and optimizing space object awareness capabilities. The first order physics of each important element (orbit behaviour, optics, etc.) are well known. However, there are many variables controlling an imaging scenario and obtaining understandable, relevant predictions can be difficult to achieve and hard to document or articulate. In addition, first order physics may be insufficient for some topics, such as the optical scattering of satellite materials, if a realistic prediction is to be achieved.

## 6.0 REFERENCES

1. D. C. Harrison and J. C. Chow, "The Space-Based Visible Sensor," Johns Hopkins APL Technical Digest, Vol. 17, No. 2, 226-236 (1996)
2. M. L. Pugh and M. J. Duggin, "Sensor Fusion for Space Situational Awareness," Proceedings of the 2007 Military Sensing Symposia National Symposium on Sensor and Data Fusion, Nellis AFB, NV, Nov. 2007.
3. J. F. Riker et al., "Satellite Imaging Experiment tracking simulation results," Proc. SPIE Vol. 2221, 235-247 (1994)
4. J. F. Riker, G. A. Crockett and R. L. Brunson, "The time-domain analysis simulation for advanced tracking (TASAT)", SPIE Vol. 1697, 297-309 (1992)
5. J. R. Maxwell, J. Beard, Bidirectional Reflectance Model Validation and Utilization, ERIM Technical Report AFAL-TR-73-303, October 1973.
6. Keith A. Bush, et al., "Polarization rendering and modelling of coherent polarized speckle background using TASAT", SPIE Vol. 3121, 142-154 (1997)
7. Keith Bush, Greg Crockett and Calvin Barnard, "Satellite discrimination from active and passive polarization signatures: simulation predictions using the TASAT satellite model", SPIE Vol. 4481, 46-57 (2002)